[5] S. L. Cotton, W. G. Scanlon, and J. Guy, "The $\kappa-\mu$ distribution applied to the analysis of fading in body to body communication channels for fire and rescue personnel," *IEEE Antennas Wireless Propag. Lett.*, vol. 7, pp. 66–69, 2008.

[6] N. Ermolova, "Moment generating functions of the generalized $\eta-\mu$ and $\kappa-\mu$ distributions and their applications to performance evaluations of communication systems," *IEEE Commun. Lett.*, vol. 12, no. 7, pp. 502–504, Jul. 2008.

[7] N. Ermolova, "Useful integrals for performance evaluation of communication systems in generalized $\eta-\mu$ and $\kappa-\mu$ fading channels," *IET Commun.*, vol. 3, no. 2, pp. 303–308, Feb. 2009.

[8] D. B. da Costa and M. D. Yacoub, "Accurate approximations to the sum of generalized random variables and applications in the performance analysis of diversity systems," *IEEE Trans. Commun.*, vol. 57, no. 5, pp. 1271–1274, May 2009.

[9] D. B. da Costa and M. D. Yacoub, "Average channel capacity for generalized fading scenarios," *IEEE Commun. Lett.*, vol. 11, no. 12, pp. 949–951, Dec. 2007.

[10] M. Milisic, M. Hamza, and M. Hadzialic, "Outage performance of L-branch maximal-ratio combiner for generalized $\kappa-\mu$ fading," in *Proc. IEEE Veh. Technol. Conf.*, Singapore, 2008, pp. 325–329.

[11] M. Milisic, M. Hamza, and M. Hadzialic, "Outage and symbol error probability performance of L-branch maximal-ratio combiner for generalized $\kappa-\mu$ fading," in *Proc. 50th Int. Symp. ELMAR*, 2008, pp. 231–236.

[12] I. Gradshteyn and I. M. Ryzhik, *Tables of Integrals, Series, and Products*, 6th ed. New York: Academic, 2000.

[13] A. Castano-Martinez and F. Lopez-Blazquez, "Distribution of a sum of weighted noncentral chi-square variables," *TEST*, vol. 14, no. 2, pp. 397–415, Dec. 2005.

[14] M.-S. Alouini and A. J. Goldsmith, "Capacity of Rayleigh fading channels under different adaptive transmission and diversity-combining techniques," *IEEE Trans. Veh. Technol.*, vol. 48, no. 4, pp. 1165–1181, Jul. 1999.

[15] K. P. Peppas, "Capacity of $\eta-\mu$ fading channels under different adaptive transmission techniques," *IET Commun.*, vol. 4, no. 5, pp. 532–539, Mar. 2010.

[16] T. Wolfram function site. [Online]. Available: http://functions.wolfram.com

[17] A. P. Prudnikov, Y. A. Brychkov, and O. I. Marichev, *Integrals and Series Volume 3: More Special Functions*, 1st ed. New York: Gordon and Breach, 1986.

[18] M. K. Simon and M. S. Alouini, *Digital Communication Over Fading Channels*, 2nd ed. New York: Wiley, 2005.

Efficient Beamforming for MIMO Relaying Broadcast Channel With Imperfect Channel Estimation

Zijian Wang, Wen Chen, *Senior Member, IEEE*, and Jun Li, *Member, IEEE*

***Abstract*—We consider a multiple-input–multiple-output (MIMO) relaying broadcast channel in downlink cellular networks, where the base station and the relay stations are both equipped with multiple antennas, and each user terminal has only a single antenna. In practical scenarios, channel estimation is imperfect at the receivers. Aiming to maximize the signal-to-interference noise ratio (SINR), at each user, we develop two robust linear beamforming schemes for the single-relay case and the multirelay case, respectively. The two proposed schemes are based on singular value decomposition (SVD), minimum mean square error (MMSE), and regularized zero forcing (RZF). Simulation results show that the proposed scheme outperforms the conventional schemes with imperfect channel estimation.**

***Index Terms*—Minimum mean square error (MMSE) receiver, multiple-input–multiple-output (MIMO) relaying broadcast, regularized zero-forcing (RZF) precoding, signal-to-interference noise ratio (SINR), singular value decomposition (SVD).**

I. Introduction

In recent years, multiple-input–multiple-output (MIMO) relay networks have drawn considerable interest due to the advantages of increasing the data rate and extending coverage in the cellular edge. The MIMO relay network with perfect channel state information (CSI) has been studied in [1] and [2]. In [1], Guan *et al.* investigated linear processing at relay for MIMO relay networks with a fairness requirement. In [2], Zhang *et al.* investigated the regularized zero-forcing (RZF) precoder at relays, which is observed to have an advantage over zero-forcing (ZF) and matched-filter (MF) precoders. However, the RZF precoder is not optimized and constantly chooses one as the regularizing factor. The MIMO relaying broadcast network has been considered in [3], where the singular value decomposition (SVD) and ZF precoder are used to the backward channels (BC) and the forward channels (FC), respectively, to optimize the joint precoding. The authors use an iterative method to show that the optimal precoding matrices always diagonalize the compound channel of the system.

All the above works consider perfect CSIs. However, perfect CSI is usually difficult to obtain for a practical system. In [4], minimum mean square error (MMSE)-based precoding has been considered in a

Manuscript received April 19, 2011; revised August 19, 2011; accepted October 19, 2011. Date of publication October 26, 2011; date of current version January 20, 2012. This work was supported in part by the National Science Foundation China under Grant 60972031, by the National 973 Project 2012CB316106 and Project 2009CB824900, by the National Huge Special Project 2012ZX03004004, by the National Key Laboratory Project W200907 and Project ISN11-01, and by Huawei Funding under Grant YBWL2010KJ013. The review of this paper was coordinated by Prof. W. A. Krzymien.

Z. Wang is with the Department of Electronic Engineering, Shanghai Jiao Tong University, Shanghai 200240, China, and also with the State Key Laboratory of Integrated Services Networks, Xidian University, Xian 710071, China (e-mail: wangzijian1786@sjtu.edu.cn).

W. Chen is with the Department of Electronic Engineering, Shanghai Jiao Tong University, Shanghai 200240, China, and also with the State Key Laboratory for Mobile Communications, Southeast University, Nanking 210096, China (e-mail: wenchen@sjtu.edu.cn).

J. Li is with the School of Electrical Engineering and Telecommunications, University of New South Wales, Sydney, NSW 2052, Australia (e-mail: jun.li@unsw.edu.au).

Digital Object Identifier 10.1109/TVT.2011.2173590

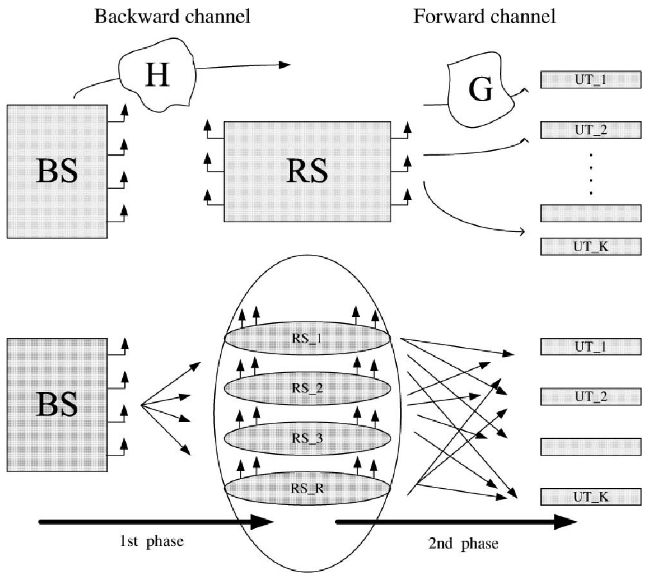

Fig. 1. MIMO relay broadcast channel with imperfect channel estimation.

multiple-antenna broadcast channel with imperfect CSI at the source. In [5], Wang *et al.* optimized QR-based beamformings with imperfect $\mathcal{R}-\mathcal{D}$ CSI due to large delay.

Works for limited feedback in MIMO relay networks are studied in [6] and [7], and those in a MIMO relaying broadcast channel are studied in [8]–[10]. In [8], Xu *et al.* further studied the impact of the feedback bits of the BC and FC on the achievable rates for the linear processing scheme in [3]. In [9], based on the MMSE criteria, robust ZF precoding are considered at the relay using the limited feedback of CSI to the relay. However, only imperfect FC is considered. In [10], Xu and Dong proposed an MMSE-based beamforming design in a MIMO relay broadcast channel with finite rate feedback.

In this paper, we study a MIMO relaying downlink broadcast channel in a wireless cellular network. Focusing on linear beamformings, we propose a robust beamforming scheme considering both imperfect channel estimation at relay and user terminals. The proposed scheme is based on SVD-RZF for the single-relay case and MMSE-RZF for the multirelay case. By maximizing the derived signal-to-interference noise ratio (SINR), we optimize the MMSE receiver and RZF precoder. Simulation results show that the proposed robust SVD-RZF and MMSE-RZF outperform other conventional beamformers.

In this paper, boldface lowercase letter and boldface uppercase letter represent vectors and matrices, respectively. Notation $\mathbb{C}^N$ denotes an $N\times 1$ complex vector. $\mathrm{tr}(\mathbf{A})$ and $\mathbf{A}^H$ denote the trace and the conjugate transpose of matrix $\mathbf{A}$, respectively. $(\mathbf{a})_k$ and $(\mathbf{A})_{j,k}$ represent the kth entry of vector $\mathbf{a}$ and the (j,k)th entry of matrix $\mathbf{A}$, respectively. $\mathbf{I}_N$ denotes the $N\times N$ identity matrix. Finally, we denote the expectation operation by $\mathrm{E}\{\cdot\}$.

II. System Model

We consider a MIMO relaying broadcast network, which consists of a base station, R fixed relays, and K user terminals, as shown in Fig. 1. The base station is equipped with M antennas, each relay is equipped with N antennas, and each user terminal only has a single antenna. It is supposed that $M,N\ge K$, so that the network can support K independent data streams. A broadcast transmission is composed of two phases. During the first phase, the base station broadcasts M precoded data streams to the relays after applying a linear precoder to the original data vector $\mathbf{s}\in\mathbb{C}^K$, where $\mathrm{E}\{\mathbf{s}\mathbf{s}^H\}=\mathbf{I}_K$. We denote the precoding matrix at the base station as $\mathbf{F}$ and suppose that the base station transmit power is P_s. Because we have $\mathrm{E}\{\mathbf{s}^H\mathbf{F}^H\mathbf{F}\mathbf{s}\}=\mathrm{tr}(\mathbf{F}^H\mathbf{F})$, the power control factor at the base station is $\rho_s=\sqrt{P_s/\mathrm{tr}(\mathbf{F}^H\mathbf{F})}$. The received signal vector at the rth relay is

$$\mathbf{y}_r=\rho_s\mathbf{H}_r\mathbf{F}\mathbf{s}+\mathbf{n}_r \tag{1}$$

where $\mathbf{H}_r\in\mathbb{C}^{N\times M}$ is the Rayleigh BC matrix of the rth relay, in which all entries are independent and identically distributed (i.i.d.) complex Gaussian distributed with zero mean and unit variance, and $\mathbf{n}_r\in\mathbb{C}^N$ is the noise vector at the relay, in which all the entries are i.i.d. complex Gaussian distributed with zero mean and variance $\sigma_1^2\mathbf{I}_N$. During the second phase, the relays all broadcast the signal vector to the user terminals after a precoding matrix $\mathbf{W}_r$. The transmit power at the relay is P_r, and the power control factor is ρ_r, where

$$\rho_r=\left(\frac{P_r}{\mathrm{tr}\left(\rho_s^2\mathbf{W}_r\mathbf{H}_r\mathbf{F}\mathbf{F}^H\mathbf{H}_r^H\mathbf{W}_r^H+\sigma_1^2\mathbf{W}_r\mathbf{W}_r^H\right)}\right)^{\frac{1}{2}}. \tag{2}$$

Denoting the received signal at the kth user terminal as y_k, the received vector at user terminals can thus be written as

$$\begin{aligned}\mathbf{y}&=[y_1,y_2,\ldots,y_K]\\&=\sum_{r=1}^{R}\rho_r\mathbf{G}_r\mathbf{W}_r(\rho_s\mathbf{H}_r\mathbf{F}\mathbf{s}+\mathbf{n}_r)+\mathbf{n}_D\end{aligned} \tag{3}$$

where $\mathbf{n}_D\in\mathbb{C}^K$ denotes the noise vector at the user terminals, in which all entries are i.i.d. Gaussian distributed with zero mean and σ_2^2 variance, and $\mathbf{G}_r$ is the Rayleigh FC matrix of the rth relay.

Considering imperfect channel estimation at both the relay and user terminals, we model the CSI as

$$\mathbf{H}_r=\widehat{\mathbf{H}}_r+e_1\mathbf{\Omega}_{1,r} \tag{4}$$

$$\left[\mathbf{g}_{1,r}^H,\mathbf{g}_{2,r}^H,\ldots,\mathbf{g}_{K,r}^H\right]^H=\mathbf{G}_r=\widehat{\mathbf{G}}_r+e_2\mathbf{\Omega}_{2,r} \tag{5}$$

where $\mathbf{g}_{k,r}^H\in\mathbb{C}^N$ is the CSI of the rth relay to the kth user channel. The entries of $\mathbf{\Omega}_{1,r}$ and $\mathbf{\Omega}_{2,r}$ are i.i.d. complex Gaussian distributed with zero mean and unit variance. $\widehat{\mathbf{H}}_r$ and $\widehat{\mathbf{G}}_r$ are the estimated CSIs, and they are independent of $\mathbf{\Omega}_{1,r}$ and $\mathbf{\Omega}_{2,r}$, respectively. e_1^2 and e_2^2 denotes the channel estimation error powers. We suppose that each user has the same channel estimation error power for simplicity.

III. Signal-to-Interference-Plus-Noise Ratio at User Terminals

Considering channel estimation errors, (3) becomes

$$\begin{aligned}\mathbf{y}=&\sum_{r=1}^{R}\rho_s\rho_r\widehat{\mathbf{G}}_r\mathbf{W}_r\widehat{\mathbf{H}}_r\mathbf{F}\mathbf{s}\\&+\sum_{r=1}^{R}\rho_s\rho_r(e_1\widehat{\mathbf{G}}_r\mathbf{W}_r\mathbf{\Omega}_{1,r}\mathbf{F}+e_2\mathbf{\Omega}_{2,r}\mathbf{W}_r\widehat{\mathbf{H}}_r\mathbf{F})\,\mathbf{s}\\&+\sum_{r=1}^{R}\rho_r(\widehat{\mathbf{G}}_r+e_2\mathbf{\Omega}_{2,r})\,\mathbf{W}_r\mathbf{n}_r+\mathbf{n}_D\end{aligned} \tag{6}$$

where we omitted the term involving e_1e_2, because we assume e_1, $e_2\ll 1$. We can write (6) as

$$\mathbf{y}=\mathbf{H}_{\mathrm{eff}}\mathbf{s}+\mathbf{n} \tag{7}$$

where $\mathbf{H}_{\mathrm{eff}}\mathbf{s}$ is the first term, and $\mathbf{n}$ is the rest terms in the right-hand side of (6). Then, the SINR at the kth user terminal can be calculated by

$$\mathrm{SINR}_k = \frac{|(\mathbf{H}_{\mathrm{eff}})_{k,k}|^2}{\sum_{j=1,j\neq k}^{K} |(\mathbf{H}_{\mathrm{eff}})_{k,j}|^2 + \mathrm{E}\{\mathbf{n}_k\mathbf{n}_k^*\}} \tag{8}$$

where

$$\begin{aligned}\mathrm{E}\{\mathbf{n}_k\mathbf{n}_k^*\} &= \sum_{r=1}^{R}\Bigg(\frac{e_1^2\rho_s^2\rho_r^2}{K}\mathrm{tr}(\mathbf{F}\mathbf{F}^H)\mathrm{tr}\left(\widehat{\mathbf{G}}_r\mathbf{W}_r\mathbf{W}_r^H\widehat{\mathbf{G}}_r^H\right)\\ &\quad + e_2^2\rho_s^2\rho_r^2\mathrm{tr}\left(\mathbf{W}_r\widehat{\mathbf{H}}_r\mathbf{F}\mathbf{F}^H\widehat{\mathbf{H}}_r^H\mathbf{W}_r^H\right)\\ &\quad + \frac{\rho_r^2\sigma_1^2}{K}\mathrm{tr}\left(\widehat{\mathbf{G}}_r\mathbf{W}_r\mathbf{W}_r^H\widehat{\mathbf{G}}_r^H\right)\\ &\quad + \rho_r^2e_2^2\sigma_1^2\mathrm{tr}\left(\mathbf{W}_r\mathbf{W}_r^H\right)\Bigg) + \sigma_2^2. \end{aligned}\tag{9}$$

In the derivation, we used the fact that $\mathrm{E}\{\mathbf{\Omega}\mathbf{A}\mathbf{\Omega}^H\} = \mathrm{tr}(\mathbf{A})\mathbf{I}_N$ for any $N\times N$ matrix $\mathbf{A}$. The expectation is taken over all distributions of $\mathbf{s}$, $\mathbf{n}_r$, $\mathbf{n}_D$, $\mathbf{\Omega}_{1,r}$, and $\mathbf{\Omega}_{2,r}$. Our aim is to find the precoding matrix at the base station and the beamforming matrix at the relay to maximize the SINR at each user terminal.

It is difficult to directly obtain the optimum closed-form solution, because the optimization problem is not convex. In fact, there is no optimal beamforming, even for perfect CSI in the MIMO relaying broadcast channels [8]. In the next section, we propose a robust beamforming scheme for two different cases, which considers imperfect channel estimations.

IV. Robust Beamforming Design

A. SVD-RZF Based Design for the Single-Relay Case

If there is only one relay, for the first phase, the transmission is similar to a point-to-point MIMO system. Therefore, we propose an SVD-based beamforming for the BC [11]. Using SVD, the imperfect BC matrix can be decomposed as

$$\widehat{\mathbf{H}} = \widehat{\mathbf{H}}_1 = \mathbf{U}\mathbf{\Sigma}\mathbf{V}^H \tag{10}$$

where $\mathbf{U}\in\mathbb{C}^{N\times N}$ and $\mathbf{V}\in\mathbb{C}^{M\times M}$ are both unitary matrices, and $\mathbf{\Sigma} = [\mathbf{\Theta}|\mathbf{0}]$, with $\mathbf{\Theta} = \mathrm{diag}\{\sqrt{\theta_1},\ldots,\sqrt{\theta_N}\}$ and $\mathbf{0}$ being an $N\times(M-N)f$ zero matrix. Then, we propose the precoding matrix $\mathbf{F}$ at the base station as the first K columns of $\mathbf{V}$ and the receiving matrix $\mathbf{W} = \mathbf{W}_1$ at the relay as $\mathbf{U}^H$. Thus, we have

$$\rho_s = \sqrt{\frac{P_s}{\mathrm{tr}(\mathbf{F}^H\mathbf{F})}} = \sqrt{\frac{P_s}{K}}. \tag{11}$$

For the second phase, the transmission is a broadcast channel. Instead of ZF or MF, in tradition, we design a robust RZF precoder for the FC. Given the imperfect FC matrix, the RZF at the relay is $\widehat{\mathbf{G}}^H(\widehat{\mathbf{G}}\widehat{\mathbf{G}}^H + \alpha\mathbf{I}_K)^{-1}$. We aim at optimizing α in the RZF precoder in terms of the SNRs of the BC and FC and the powers of channel estimation errors e_1^2 and e_2^2. Since the power penalty problem of ZF mostly exists in the case $N = K$ [12], we assume that $N = K$. Generally, a nonzero α will bring interference but can reduce the power penalty. To optimize α, we need to derive the SINR in terms of α at each user. In the following, we will see that α can be optimized based on the SINR expressed by the eigenvalues of the instantaneous CSI at each user terminal, and for the large-K case, the α is independent of the instantaneous CSI. For SVD-RZF, we have

$$\mathbf{F} = \mathbf{V} \tag{12}$$

$$\mathbf{W} = \mathbf{W}_1 = \widehat{\mathbf{G}}^H(\widehat{\mathbf{G}}\widehat{\mathbf{G}}^H + \alpha\mathbf{I}_k)^{-1}\mathbf{U}^H. \tag{13}$$

In the following derivation, we use the decomposition

$$\widehat{\mathbf{G}}\widehat{\mathbf{G}}^H = \mathbf{Q}\,\mathrm{diag}\{\lambda_1,\ldots,\lambda_K\}\mathbf{Q}^H. \tag{14}$$

Substituting (13) and (14) into (2), we have the power control factor as

$$\rho_s = \left(\frac{P_s}{K}\right)^{\frac{1}{2}} \tag{15}$$

and we have (16) and (17), shown at the bottom of the page.

Substituting (12) and (13) into (9), through some manipulations, we have the power of effective noise, i.e.,

$$\begin{aligned}N(\theta,\lambda) &= \left(\rho_s^2\rho_r^2e_1^2 + \rho_r^2\frac{\sigma_1^2}{K}\right)\sum\frac{\lambda^2}{(\lambda+\alpha)^2}\\ &\quad + \left(\frac{1}{K}\rho_s^2\rho_r^2e_2^2\sum\theta + \rho_r^2e_2^2\sigma_1^2\right)\sum\frac{\lambda}{(\lambda+\alpha)^2} + \sigma_2^2\end{aligned} \tag{18}$$

where, in the derivation, we have taken expectation over unitary matrix $\mathbf{Q}$. The received data signal vector at the user terminals can be calculated as

$$\rho_s\rho_r\widehat{\mathbf{G}}\mathbf{W}\widehat{\mathbf{H}}\mathbf{F}\mathbf{s} = \rho_s\rho_r\widehat{\mathbf{G}}\widehat{\mathbf{G}}^H(\widehat{\mathbf{G}}\widehat{\mathbf{G}}^H + \alpha\mathbf{I}_k)^{-1}\mathbf{\Theta}\mathbf{s}. \tag{19}$$

From the preceding expression, we see that the effective channel matrix is not diagonal when α is not zero. Thus, the received signal by

$$\begin{aligned}\rho_r &= \left(\frac{P_r}{\mathrm{tr}\left(\widehat{\mathbf{G}}\widehat{\mathbf{G}}^H(\widehat{\mathbf{G}}\widehat{\mathbf{G}}^H + \alpha\mathbf{I}_k)^{-2}\left(\rho_s^2\mathbf{\Theta}^2 + \rho_s^2e_1^2\mathbf{\Omega}_1\mathbf{\Omega}_1^H + \sigma_1^2\mathbf{I}_k\right)\right)}\right)^{\frac{1}{2}}\\ &= \left(\frac{P_r}{\left(\frac{P_s}{K^2}\sum\theta + e_1^2P_s + \sigma_1^2\right)\sum\frac{\lambda}{(\lambda+\alpha)^2}}\right)^{\frac{1}{2}}\end{aligned} \tag{16}$$

$$\mathrm{SINR} \xrightarrow{w.p.} \frac{\frac{P_s}{M}\left(R\mathcal{E}_1^\theta\mathcal{E}_1^\lambda\right)^2}{\frac{P_sR(M-1)}{M^2}\mathcal{E}_3^\theta\mathcal{E}_3^\lambda + (e_1^2P_s + \sigma_1^2)R\mathcal{E}_2^\theta\mathcal{E}_3^\lambda + P_sRe_2^2\mathcal{E}_3^\theta\mathcal{E}_2^\lambda + e_2^2\sigma_1^2RM\mathcal{E}_2^\theta\mathcal{E}_2^\lambda + \sigma_2^2\rho_r^{-2}} \tag{17}$$

a user terminal consists of the desired signal and the interference from other users' signal. To divide the interference from the desired signal, we introduce the following two lemmas:

Lemma 1: If $\mathbf{A} = \mathbf{Q}\mathbf{\Lambda}\mathbf{Q}^H$, then $\mathrm{E}\{(\mathbf{A})_{k,k}^2\} = (1/K(K+1))((\sum\lambda)^2 + \sum\lambda^2) \triangleq \mu(\lambda)$.The proof of Lemma 1 can be directly obtained in [12].

Lemma 2: If $\mathbf{A} = \mathbf{Q}\mathbf{\Lambda}\mathbf{Q}^H$, then $\mathrm{E}\{(\mathbf{A})_{k,j}^2\} = (1/(K-1)(K+1))\sum\lambda^2 - (1/(K-1)K(K+1))(\sum\lambda)^2 \triangleq \nu(\lambda)$, for $k \neq j$.

Proof: Because $\mathbf{A}$ is a conjugate symmetric matrix, we have

$$\begin{aligned}\mathrm{E}\left\{\sum_{j=1,j\neq k}^{K} |(\mathbf{A})_{k,j}|^2\right\} + \mathrm{E}\left\{(\mathbf{A})_{k,k}^2\right\} &= \mathrm{E}\left\{(\mathbf{A}\mathbf{A}^H)_{k,k}\right\} \\ &= \mathrm{E}\left\{\left(\mathbf{Q}\mathbf{\Lambda}^2\mathbf{Q}^H\right)_{k,k}\right\} \\ &= \frac{1}{K}\sum\lambda^2. \end{aligned} \tag{20}$$

Since $\mathrm{E}\{(\mathbf{A})_{k,j}^2\}$ are all equal for $j \neq k$, we have

$$\begin{aligned}\mathrm{E}\left\{|(\mathbf{A})_{k,j}|^2\right\} &= \frac{1}{(K-1)}\left(\frac{1}{K}\sum\lambda^2 - \mathrm{E}\{(\mathbf{A})_{k,k}^2\}\right) \\ &= \frac{1}{(K-1)(K+1)}\sum\lambda^2 \\ &\quad - \frac{1}{(K-1)K(K+1)}(\sum\lambda)^2. \end{aligned} \tag{21}$$

■

Therefore, for user k, if we denote $\mathbf{A} = \widehat{\mathbf{G}}\widehat{\mathbf{G}}^H(\widehat{\mathbf{G}}\widehat{\mathbf{G}}^H + \alpha\mathbf{I}_k)^{-1}$, we can calculate the power of desired signal as

$$\mathrm{E}\left\{\|\mathbf{A}_{k,k}\theta_k(\mathbf{s})_k\|^2\right\} = \rho_s^2\rho_r^2\theta_k\mu\left(\frac{\lambda}{\lambda+\alpha}\right). \tag{22}$$

The power of interference is

$$\begin{aligned}&\mathrm{E}\left\{\left\|\sum_{j=1,j\neq k}^{K}\mathbf{A}_{k,j}\theta_j(\mathbf{s})_j\right\|^2\right\} \\ &\qquad = \rho_s^2\rho_r^2\left(\sum_{j=1,j\neq k}^{K}\theta_j\right)\nu\left(\frac{\lambda}{\lambda+\alpha}\right). \end{aligned} \tag{23}$$

Finally, the SINR at user k is

$$\mathrm{SINR}_k = \frac{\rho_s^2\rho_r^2\theta_k\mu\left(\frac{\lambda}{\lambda+\alpha}\right)}{\rho_s^2\rho_r^2\left(\sum_{j=1,j\neq k}^{K}\theta_j\right)\nu\left(\frac{\lambda}{\lambda+\alpha}\right) + N(\theta,\lambda)}. \tag{24}$$

Note that, in the preceding expression, the SINR is based on the eigenvalue of instantaneous imperfect CSIs. To maximize the SINR expression, we introduce the following lemma, which is a conclusion of [12, App. B]:

Lemma 3:

$$\mathrm{SINR}(\alpha) = \frac{A\left(\sum\frac{\lambda}{\lambda+\alpha}\right)^2 + B\sum\frac{\lambda^2}{(\lambda+\alpha)^2}}{C\sum\frac{\lambda}{(\lambda+\alpha)^2} + D\sum\frac{\lambda^2}{(\lambda+\alpha)^2} + E\left(\sum\frac{\lambda}{\lambda+\alpha}\right)^2} \tag{25}$$

for large K is maximized by $\alpha = C/D$.

Using Lemma 3, we finally get the optimized

$$\alpha_{\mathrm{SVD-RZF,opt}} = \frac{\frac{e_2^2\sum\theta}{K} + \frac{e_2^2\sigma_1^2 K}{P_s} + \frac{\sigma_2^2}{P_r}\left(\frac{\sum\theta}{K} + Ke_1^2 + \frac{\sigma_1^2 K}{P_s}\right)}{\frac{\sum\theta_j}{(K-1)(K+1)} + e_1^2 + \frac{\sigma_1^2}{P_s}}. \tag{26}$$

For large K, we have

$$\begin{aligned}\alpha_{\mathrm{SVD-RZF,opt}} &\approx \frac{\frac{e_2^2K^2}{K} + \frac{e_2^2\sigma_1^2K}{P_s} + \frac{\sigma_2^2}{P_r}\left(\frac{K^2}{K} + Ke_1^2 + \frac{\sigma_1^2K}{P_s}\right)}{\frac{K(K-1)}{(K-1)(K+1)} + e_1^2 + \frac{\sigma_1^2}{P_s}} \\ &\approx K\left(\frac{e_2^2 + e_2^2\sigma_1^2/P_s}{1 + e_1^2 + \sigma_1^2/P_s} + \sigma_2^2/P_r\right). \end{aligned} \tag{27}$$

B. MMSE-RZF-Based Design for Multirelay Case

Although SVD is advantageous, it can only be implemented in the single-relay case. For the multirelay case, the relays have to work in a cooperative mode to diagonalize the channel as SVD, or the base station needs the CSI of all the backward channels, which will lead to considerable delay. Therefore, for the multirelay case, we propose another beamforming scheme, which is based on MMSE-RZF, instead of SVD-RZF.

It is known that the MMSE receiver is widely used in point-to-point MIMO systems. The MMSE receiver can be viewed as a duality of the RZF precoder, where the difference is that the RZF precoder is frequently used in multiantenna multiuser communication. Our main idea is to obtain the optimal regularizing factor in the MMSE receiver to reduce the effect of the channel estimation error of the backward channels.

The MMSE receiver at the rth relay is $(\widehat{\mathbf{H}}_r^H\widehat{\mathbf{H}}_r + \alpha^{\mathrm{MMSE}})^{-1}\widehat{\mathbf{H}}_r^H$. For the same reason as RZF, the MMSE receiver is most superior to other linear receivers (e.g., ZF) when $M = N$. Thus, we consider $M = N = K$ for the multirelay case. Because the aim of the MMSE receiver is to reduce the effect of the channel estimation error of the BC, we optimize α^{MMSE} by idealizing the FCs as Gaussian channels, i.e., the FC is considered as $\widehat{\mathbf{G}}_r = \mathbf{G}_r = \mathbf{I}_N$.

In the following analysis, we use the decompositions:

$$\widehat{\mathbf{H}}_r^H\widehat{\mathbf{H}}_r = \mathbf{P}_r\mathrm{diag}\{\theta_{r,1},\ldots,\theta_{r,N}\}\mathbf{P}_r^H \tag{28}$$

$$\widehat{\mathbf{G}}_r\widehat{\mathbf{G}}_r^H = \mathbf{Q}_r\mathrm{diag}\{\lambda_{r,1},\ldots,\lambda_{r,N}\}\mathbf{Q}_r^H \tag{29}$$

where $\mathbf{P}_r$ and $\mathbf{Q}_r$ are unitary matrices. For the rth relay, the signal vector processed by an MMSE receiver is

$$\begin{aligned}\mathbf{v}_r &= \rho_r\left(\widehat{\mathbf{H}}_r^H\widehat{\mathbf{H}}_r + \alpha^{\mathrm{MMSE}}\mathbf{I}_M\right)^{-1}\widehat{\mathbf{H}}_r^H\mathbf{r}_r \\ &= \rho_r\left(\widehat{\mathbf{H}}_r^H\widehat{\mathbf{H}}_r + \alpha^{\mathrm{MMSE}}\mathbf{I}_M\right)^{-1}\widehat{\mathbf{H}}_r^H\widehat{\mathbf{H}}_r\mathbf{s} \\ &\quad + \rho_r e_1\left(\widehat{\mathbf{H}}_r^H\widehat{\mathbf{H}}_r + \alpha^{\mathrm{MMSE}}\mathbf{I}_M\right)^{-1}\widehat{\mathbf{H}}_r^H\mathbf{\Omega}_{1,r}\mathbf{s} \\ &\quad + \rho_r\left(\widehat{\mathbf{H}}_r^H\widehat{\mathbf{H}}_r + \alpha^{\mathrm{MMSE}}\mathbf{I}_M\right)^{-1}\widehat{\mathbf{H}}_r^H\mathbf{n}_r. \end{aligned} \tag{30}$$

Using similar manipulations with the single-relay case, the SINR of the kth user's data at the rth relay is

$$\mathrm{SINR}_{r,k}^R = \frac{\frac{P_s}{M}\mu\left(\frac{\theta_r}{\theta_r+\alpha^{\mathrm{MMSE}}}\right)}{\frac{P_s(M-1)}{M}\nu\left(\frac{\theta_r}{\theta_r+\alpha^{\mathrm{MMSE}}}\right) + \frac{e_1^2P_s+\sigma_1^2}{M}\sum\frac{\theta_r}{(\theta_r+\alpha^{\mathrm{MMSE}})^2}}. \tag{31}$$

At the destination, the received vector is from all the R relays. Thus, the desired signal is scaled by R^2, and the interference and the noise inherited from the relays are scaled by R. Therefore, by idealizing the FCs, we have the SINR of the kth stream as (32), shown at the bottom of the next page, where power control factor ρ_r at the relay normalizes the noise at the destination. We use the same ρ_r for all the relays for simplicity of analysis by taking expectation to the denominator in (2). Using Lemma 3, we obtain

$$\alpha^{\mathrm{MMSE,opt}} = \frac{\frac{P_s e_1^2+\sigma_1^2}{P_r}\sigma_2^2 + R\frac{P_s e_1^2+\sigma_1^2}{M}}{\frac{P_s\sigma_2^2}{MP_r} + R\frac{P_s(M-1)}{M}\frac{1}{(M-1)(M+1)}}$$

$$= \left(e_1^2 + \frac{\sigma_1^2}{P_s}\right)\frac{M+\frac{P_r R}{\sigma_2^2}}{1+\frac{P_r R}{(M+1)\sigma_2^2}}. \quad (33)$$

To obtain the optimal α^{RZF}, we need to derive the asymptotic SINR of the system. Again, we separate the desired signals from the interference and the noise and finally derive the SNR at the kth user terminal as

$$\mathrm{SINR}_k^D = \frac{\frac{P_s}{M}\left|(\mathbf{H}_{\mathcal{SD}})_{k,k}\right|^2}{\frac{P_s}{M}\sum_{j=1,j\neq k}^{K}\left|(\mathbf{H}_{\mathcal{SD}})_{j,k}\right|^2 + N(\mathbf{G}_r,\mathbf{H}_r)} \quad (34)$$

where

$$\mathbf{H}_{\mathcal{SD}} = \sum_{r=1}^{R}\rho_r\widehat{\mathbf{G}}_r\mathbf{W}_r\widehat{\mathbf{H}}_r \quad (35)$$

$$N(\mathbf{G}_r,\mathbf{H}_r) = \left(e_1^2P_s+\sigma_1^2\right)\sum_{r=1}^{R}\left\|\rho_r(\widehat{\mathbf{G}}_r\mathbf{W}_r)_k\right\|^2 + \frac{P_s e_2^2}{M}\sum_{r=1}^{R}\rho_r^2\mathrm{tr}\left(\mathbf{W}_r\widehat{\mathbf{H}}_r\widehat{\mathbf{H}}_r^H\mathbf{W}_r^H\right) + e_2^2\sigma_1^2\sum_{r=1}^{R}\rho_r^2\mathrm{tr}\left(\mathbf{W}_r\mathbf{W}_r^H\right)+\sigma_2^2. \quad (36)$$

For the case of a large R, using the Law of Large Number, we have (37) and (38), shown at the bottom of the page, where, in (a), we approximate $\mathrm{E}\{|(\mathbf{Q}_r)_{i,k}|^2|(\mathbf{Q}_r)_{l,k}|^2\} \approx (1/M^2)$. In fact, this

$$\mathrm{SINR}_k^D \approx \frac{\frac{P_sR^2}{M}\mu\left(\frac{\theta}{\theta+\alpha^{\mathrm{MMSE}}}\right)}{R\frac{P_s(M-1)}{M}\nu\left(\frac{\theta}{\theta+\alpha^{\mathrm{MMSE}}}\right) + R\frac{e_1^2P_s+\sigma_1^2}{M}\sum\frac{\theta}{\left(\theta+\alpha^{\mathrm{MMSE}}\right)^2} + \sigma_2^2\rho_r^{-2}} \quad (32)$$

$$\begin{aligned}
\left|(\mathbf{H}_{\mathcal{SD}})_{i,i}\right| &\xrightarrow{w.p.} R\rho_r\left(\mathrm{E}\left\{(\widehat{\mathbf{G}}_r\mathbf{W}_r\widehat{\mathbf{H}}_r)_{i,i}\right\}\right)\\
&= R\rho_r\mathrm{E}\left\{\left(\mathbf{Q}_r\frac{\mathbf{\Lambda}_r}{\mathbf{\Lambda}_r+\alpha^{\mathrm{RZF}}\mathbf{I}_M}\mathbf{Q}_r^H\mathbf{P}_r\frac{\mathbf{\Theta}_r}{\mathbf{\Theta}_r+\alpha^{\mathrm{MMSE}}\mathbf{I}_N}\mathbf{P}_r^H\right)_{i,i}\right\}\\
&= R\rho_r\mathrm{E}\left\{\left(\mathbf{Q}_r\frac{\mathbf{\Lambda}_r}{\mathbf{\Lambda}_r+\alpha^{\mathrm{RZF}}\mathbf{I}_M}\mathbf{Q}_r^H\right)_{m,m}\right\}\\
&\quad\times\mathrm{E}\left\{\left(\mathbf{P}_r\frac{\mathbf{\Theta}_k}{\mathbf{\Theta}_r+\alpha^{\mathrm{MMSE}}\mathbf{I}_N}\mathbf{P}_r^H\right)_{n,n}\right\}\\
&= \frac{R\rho_r}{MN}\mathrm{E}\left\{\sum\frac{\theta_r}{\theta_r+\alpha^{\mathrm{MMSE}}}\right\}\mathrm{E}\left\{\sum\frac{\lambda_r}{\lambda_r+\alpha^{\mathrm{RZF}}}\right\}\\
&= R\rho\mathrm{E}\left\{\frac{\theta}{\theta+\alpha^{\mathrm{MMSE}}}\right\}\mathrm{E}\left\{\frac{\lambda}{\lambda+\alpha^{\mathrm{RZF}}}\right\}
\end{aligned} \quad (37)$$

$$\begin{aligned}
&\left|(\mathbf{H}_{\mathcal{SD}})_{(i,j)}\right|^2\\
&= \left|\left(\sum_{r=1}^{R}\mathbf{Q}_r\frac{\mathbf{\Lambda}_r}{\mathbf{\Lambda}_r+\alpha^{\mathrm{RZF}}\mathbf{I}_M}\mathbf{Q}_r^H\mathbf{P}_r\frac{\mathbf{\Theta}_r}{\mathbf{\Theta}_r+\alpha^{\mathrm{MMSE}}\mathbf{I}_N}\mathbf{P}_r^H\right)_{(i,j)}\right|^2\\
&= \sum_r\left|(\mathbf{Q}_r)_{i,k}\frac{\lambda_{r,k}}{\lambda_{r,k}+\alpha^{\mathrm{MMSE}}}(\mathbf{Q}_r)_{l,k}^*(\mathbf{P}_r)_{l,m}\frac{\theta_{r,m}}{\theta_{r,m}+\alpha^{\mathrm{RZF}}}(\mathbf{Q}_r)_{j,m}^*\right|^2\\
&\overset{(a)}{\approx}\sum_{k,m,n,r}\frac{1}{M^4}\left(\frac{\lambda_{r,k}}{\lambda_{r,k}+\alpha^{\mathrm{RZF}}}\right)^2\left(\frac{\theta_{r,k}}{\theta_{r,k}+\alpha^{\mathrm{MMSE}}}\right)^2\\
&\xrightarrow{w.p.}\frac{R}{M}\mathrm{E}\left\{\frac{\theta^2}{(\theta+\alpha^{\mathrm{MMSE}})^2}\right\}\mathrm{E}\left\{\frac{\lambda^2}{(\lambda+\alpha^{\mathrm{RZF}})^2}\right\}
\end{aligned} \quad (38)$$

expectation is $(2/M(M+1))$ if $i=1$ or $(1/M(M+1))$ if $i \neq 1$ [12]. Here, we denote λ and θ without subscript r for simplicity, because all the channels for different relays are i.i.d. Let us define the expectations as $\mathcal{E}_1^\theta \triangleq \mathrm{E}\{\theta/(\theta+\alpha^{\mathrm{MMSE}})\}$, $\mathcal{E}_2^\theta \triangleq \mathrm{E}\{\theta/(\theta+\alpha^{\mathrm{MMSE}})^2\}$, $\mathcal{E}_3^\theta \triangleq \mathrm{E}\{\theta^2/(\theta+\alpha^{\mathrm{MMSE}})^2\}$, $\mathcal{E}_1^\lambda \triangleq \mathrm{E}\{\lambda/(\lambda+\alpha^{\mathrm{RZF}})\}$, $\mathcal{E}_2^\lambda \triangleq \mathrm{E}\{\lambda/(\lambda+\alpha^{\mathrm{RZF}})^2\}$, and $\mathcal{E}_3^\lambda \triangleq \mathrm{E}\{\lambda^2/(\lambda+\alpha^{\mathrm{RZF}})^2\}$. Substituting (36)–(38) into (34), we obtain the asymptotic SINR at each user terminal as (39), shown at the bottom of the page. The calculation of (36) can follow the same line as (37). Generally, the expectations in the asymptotic SINR are difficult. Fortunately, if we approximate the expectations by the arithmetic mean, for large R, then the asymptotic SINR can be maximized by using Lemma 3. Finally, we obtain

$$\alpha^{\mathrm{RZF,opt}} \approx \frac{\left(P_s R e_2^2 + \frac{\sigma_2^2 P_s}{P_r}\right)\mathcal{E}_3^\theta + \left(e_2^2\sigma_1^2 RM + \frac{(e_1^2 P_s + \sigma_1^2)M}{P_r}\right)\mathcal{E}_2^\theta}{(e_1^2 P_s + \sigma_1^2)\, R\mathcal{E}_2^\theta + \frac{P_s R}{M}\mathcal{E}_3^\theta}. \tag{40}$$

Note that, although we maximize the SINR for large K and large R for the multirelay case, we will see from the numerical simulation that the obtained beamforming is robust enough for small K and R when channel estimation error occurs.

V. Simulation Results

In this section, numerical simulations have been carried out. For the single-relay case, we compare the SINR at each user terminal of the robust SVD-RZF beamforming with SVD-ZF and SVD-MF in [3], MMSE-RZF in [9], and two other relative beamforming schemes such as ZF-ZF and SVD-RZF for references. For MMSE-RZF, $\alpha_{\mathrm{MMSE}} = K\sigma_1^2/P_s$, and $\alpha_{\mathrm{RZF}} = K\sigma_2^2/P_r$. We also consider the robust MMSE-RZF proposed for the multirelay case for $R=1$. For the multirelay case, we compare with the conventional MMSE-RZF and ZF-ZF. All the results are averaged over 10 000 different channel realizations.

A. SINR Performances for the Single-Relay Case

Fig. 2 shows the SINRs of different beamforming schemes versus the SNR of the BC. We observe that the proposed robust SVD-RZF beamforming has consistent advantage over others. Robust MMSE-RZF underperforms robust SVD-RZF and SVD-MF, which shows the superiority of SVD. Fig. 3 shows the SINRs versus the SNR of the FC. The SINR of SVD-RZF even falls and converges to SVD-ZF when the SNR of the FC increases, because α converges to zero, which should remain nonzero if estimation error is considered. Fig. 4 shows the SINRs versus the number of users K. We see that the robust SVD-RZF also outperforms others when K is small. The advantage of robust SVD-RZF comes from the fact that the SVD beamforming outperforms robust MMSE receiver, although the former ignores the estimation error. For the broadcast phase, the robust RZF compensates well the estimation error compared with ZF and RZF.

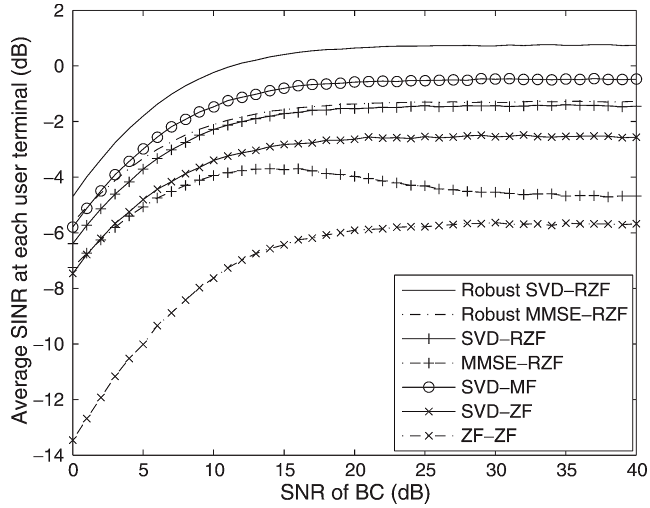

Fig. 2. SINRs at each user terminal for different beamforming schemes versus the SNR of the BC in the single-relay case. $P_r/\sigma_2^2 = 20$ dB, $e_1^2 = 0.2$, and $e_2^2 = 0.2$. The robust MMSE-RZF and MMSE-RZF will change with the SNR of the BC due to the regularizing factor in the MMSE receiver.

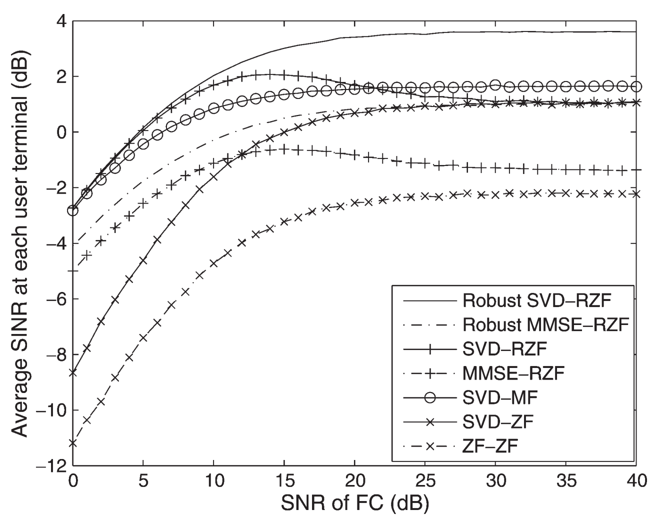

Fig. 3. SINRs at each user terminal for different beamforming schemes versus the SNR of FC in the single-relay case. $P_s/\sigma_1^2 = 20$ dB, $e_1^2 = 0.1$, and $e_2^2 = 0.1$. The beamformings with RZF will change with the SNR of FC due to the regularizing factor.

B. SINR Performances for the Multirelay Case

For multirelay case, where SVD cannot be implemented, we only compare the proposed robust MMSE-RZF with MMSE-RZF and ZF-ZF. Fig. 5 shows the average SINR performances versus the power of channel estimation error ($e_1^2 = e_2^2$). This is because α^{MMSE} and α^{RZF} increase with e_1 and e_2, respectively, to decrease the effect of the estimation error. This can be directly seen from Fig. 6. Fig. 7 shows the sum rate performances versus the number of relays R with perfect and imperfect channel estimation. We see that all sum rates

$$\begin{aligned}\rho_r^{-2} &= \frac{1}{P_r} \times \mathrm{E}\left\{\frac{P_s}{M}\mathrm{tr}\left(\mathbf{F}_k(\widehat{\mathbf{H}}_k\widehat{\mathbf{H}}_k^H + e_1^2\mathbf{\Omega}_{1,k}\mathbf{\Omega}_{1,k}^H)\mathbf{F}_k^H\right) + \sigma_1^2\mathrm{tr}\left(\mathbf{F}_k\mathbf{F}_k^H\right)\right\} \\ &= \frac{P_s}{P_r}\mathcal{E}_3^\theta\mathcal{E}_2^\lambda + \frac{(e_1^2P_s+\sigma_1^2)\,M}{P_r}\mathcal{E}_2^\theta\mathcal{E}_2^\lambda \end{aligned} \tag{39}$$

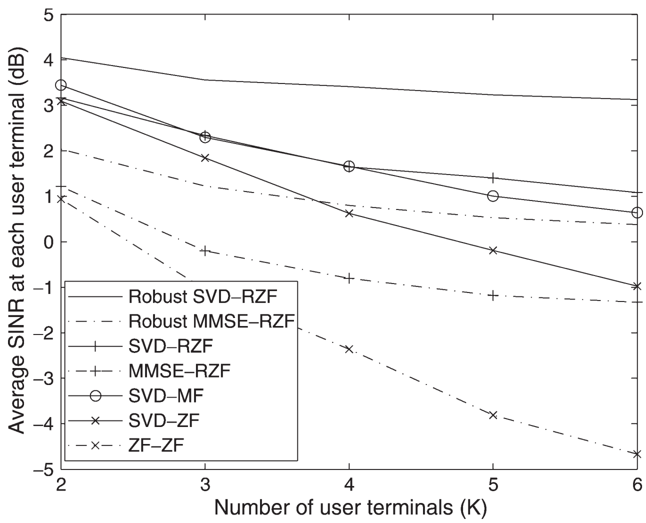

Fig. 4. SINRs at each user terminal for different beamforming schemes versus the number of users K in the single-relay case. $P_s/\sigma_1^2 = 20$ dB, $P_r/\sigma_2^2 = 20$ dB, and $e_1^2 = e_2^2 = 0.1$.

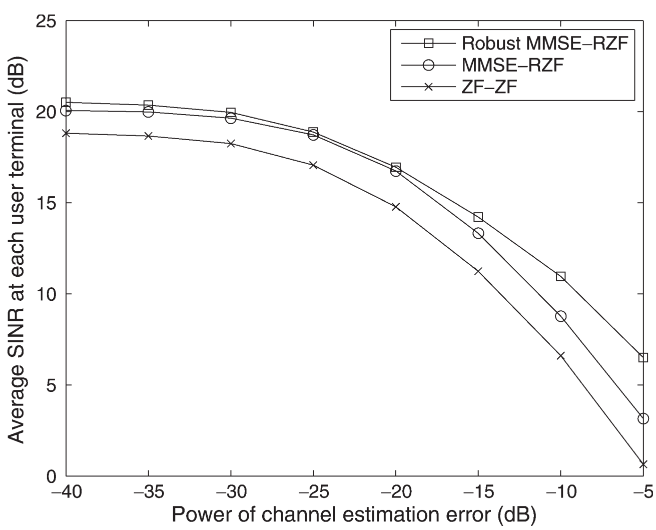

Fig. 5. SINRs at each user terminal for different beamforming schemes versus the power of channel estimation error in the multirelay case. $P_s/\sigma_1^2 = P_r/\sigma_2^2 = 20$ dB, $e_1 = e_2$, and $R = 10$. The power of channel estimation error is $e_1^2 = e_2^2$.

logarithmically increases with R, and the superior of robust MMSE-RZF increases when channel estimation is imperfect or the number of relays increases. This is because, comparing with conventional MMSE-RZF, the robust one considers both imperfect channel estimation and multiple relays.

VI. Conclusion

In this paper, we have proposed robust SVD-RZF and robust MMSE-RZF beamformers, which consider imperfect channel estimation for a multiuser downlink MIMO relaying network. For the single-relay case, the SINR expression at the user terminals based on the eigenvalue of the BC and FC matrix has been derived to obtain the optimized RZF. For the multirelay case, the asymptotic SINR has been derived to obtain the optimized MMSE and RZF. Simulation results have shown that the proposed robust SVD-RZF and MMSE-RZF outperform conventional schemes for various conditions of the SNR of channels; power of estimation errors; and number of antennas, users, and relays.

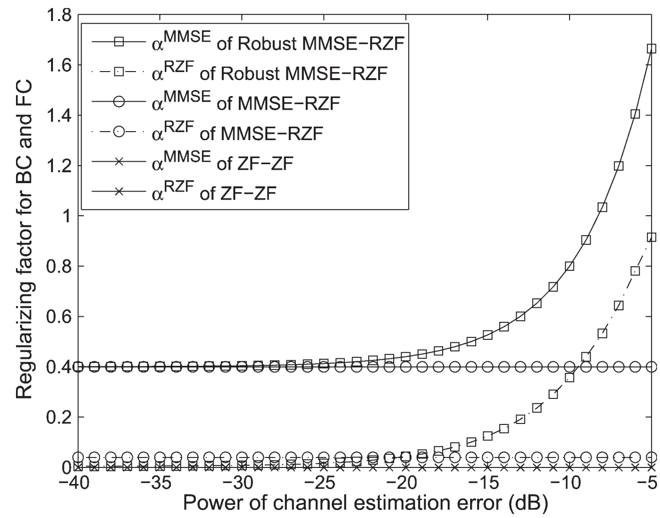

Fig. 6. α^{MMSE} and α^{RZF} for different beamforming schemes versus the power of channel estimation error in the multirelay case. $P_s/\sigma_1^2 = 10$ dB, $P_r/\sigma_2^2 = 20$ dB, $e_1 = e_2$, and $R = 10$.

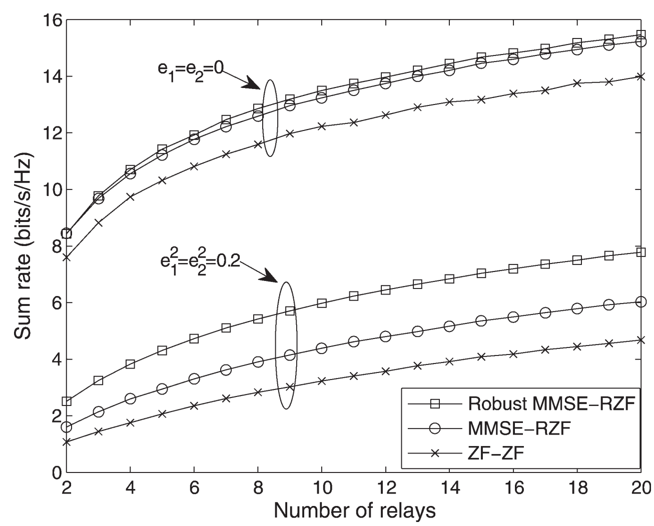

Fig. 7. Sum rates for different beamforming schemes versus the number of relays R in the multirelay case with perfect channel estimation and channel estimation errors. $P_s/\sigma_1^2 = P_r/\sigma_2^2 = 20$ dB, $e_1 = e_2 = 0$, or $e_1^2 = e_2^2 = 0.2$. The sum rate are averaged by $0.5K \log_2(1 + \mathrm{SINR}_k)$. The factor 0.5 is due to the two time slot transmissions.

References

[1] W. Guan, H.-W. Luo, and W. Chen, "Linear relaying scheme for MIMO relay system with QoS requirements," *IEEE Signal Process. Lett.*, vol. 15, pp. 697–700, 2008.

[2] Y. Zhang, H.-W. Luo, and W. Chen, "Efficient relay beamforming design with SIC detection for Dual-Hop MIMO relay networks," *IEEE Trans. Veh. Technol.*, vol. 59, no. 8, pp. 4192–4197, Oct. 2010.

[3] W. Xu, X.-D. Dong, and W.-S. Lu, "Joint optimization for source and relay precoding under multiuser MIMO downlink channels," in *Proc. IEEE ICC*, 2010, pp. 1–5.

[4] A. D. Dabbagh and D. J. Love, "Multiple antenna MMSE based downlink precoding with quantized feedback or channel mismatch," *IEEE Trans. Commun.*, vol. 56, no. 11, pp. 1859–1868, Nov. 2008.

[5] Z. Wang, W. Chen, F. Gao, and J. Li, "Capacity performance of efficient relay beamformings for dual-hop MIMO multirelay networks with

imperfect $\mathcal{R} - \mathcal{D}$ CSI at relays," *IEEE Trans. Veh. Technol.*, vol. 60, no. 6, pp. 2608–2619, Jul. 2011.

[6] Y. Huang, L. Yang, M. Bengtsson, and B. Ottersten, "A limited feedback joint precoding for amplify-and forward relaying," *IEEE Trans. Signal Process.*, vol. 58, no. 3, pp. 1347–1357, Mar. 2010.

[7] B. Khoshnevis, W. Yu, and R. Adve, "Grassmannian beamforming for MIMO amplity-and-forward relaying," *IEEE J. Sel. Areas Commun.*, vol. 26, no. 8, pp. 1397–1407, Oct. 2008.

[8] W. Xu, X.-D. Dong, and W.-S. Lu, "MIMO relaying broadcast channels with linear precoding and quantized channel state information feedback," *IEEE Trans. Signal Process.*, vol. 58, no. 10, pp. 5233–5245, Oct. 2010.

[9] B. Zhang, Z.-Q. He, K. Niu, and L. Zhang, "Robust linear beamforming for MIMO relay broadcast channel with limited feedback," *IEEE Signal Process. Lett.*, vol. 17, no. 2, pp. 209–212, Feb. 2010.

[10] W. Xu and X.-D. Dong, "MMSE relaying design for multi-antenna two-hop downlinks with finite-rate feedback," in *Proc. IEEE GlobalCom*, 2010, pp. 1–5.

[11] E. Telatar, "Capacity of multi-antenna Gaussian channels," *Euro. Trans. Telecommun.*, vol. 10, no. 6, pp. 585–596, Nov./Dec. 1999.

[12] C. Peel, B. Hochwald, and A. Swindlehurst, "Vector-perturbation technique for near-capacity multiantenna multiuser communication—Part I: Channel inversion and regularization," *IEEE Trans. Commun.*, vol. 53, no. 1, pp. 195–202, Jan. 2005.

k-Connectivity Analysis of One-Dimensional Linear VANETs

Zhongjiang Yan, *Student Member, IEEE*, Hai Jiang, *Member, IEEE*, Zhong Shen, *Member, IEEE*, Yilin Chang, and Lijie Huang

***Abstract*—In a 1-D linear vehicular ad hoc network (1-DL-VANET), some vehicles may leave the network (e.g., at highway exits), which may make the 1-DL-VANET disconnected. Thus, it is important to analyze the connectivity of the 1-DL-VANET. When removal of any $(k-1)$ arbitrary nodes from a network does not disconnect the network, the network is said to be k-connected. In this paper, we investigate the k-connectivity of the 1-DL-VANET. Sufficient and necessary conditions are derived for the 1-DL-VANET to be k-connected, and based on this, a method is provided, with the help of matrix decomposition, to obtain expression of the probability of the 1-DL-VANET being k-connected. The expectation of the maximum number of tolerable vehicle departures is also derived. Simulation results confirm the accuracy of our analysis and indicate that the expectation of the maximum number of tolerable vehicle departures almost linearly increases with the total number of vehicles.**

***Index Terms*—k-connectivity, 1-D linear networks, vehicular ad hoc networks (VANETs).**

Manuscript received March 26, 2011; revised July 13, 2011 and September 20, 2011; accepted November 12, 2011. Date of publication November 22, 2011; date of current version January 20, 2012. This work was supported by the Natural Science and Engineering Research Council of Canada under a discovery grant and in part by the National Natural Science Foundation of China under Project 61172069. The review of this paper was coordinated by Dr. F. Bai.

Z. Yan was a visiting student with the Department of Electrical and Computer Engineering, University of Alberta, Edmonton, AB T6G 2V4, Canada. He is now with the State Key Laboratory of Integrated Service Network, Xidian University, Xi'an 710071, China (e-mail: yangelc@msn.com).

H. Jiang and L. Huang are with the Department of Electrical and Computer Engineering, University of Alberta, Edmonton, AB T6G 2V4, Canada (e-mail: hai1@ualberta.ca; lijie@ualberta.ca).

Z. Shen and Y. Chang are with the State Key Laboratory of Integrated Service Network, Xidian University, Xi'an 710071, China (e-mail: z.shen.xidian@gmail.com; ylchang@gmail.com).

Digital Object Identifier 10.1109/TVT.2011.2176969

I. Introduction

A vehicular ad hoc network (VANET) consists of a group of moving vehicles and probably a fixed infrastructure (such as roadside units), supporting intervehicle communications, and vehicle-to-infrastructure communications. Typical information transmitted in a VANET includes safety messages (such as accident notifications, road condition warnings, and emergency braking alarms) and interactive communications (such as instant message and online games). In this work, we consider intervehicle communications among a group of vehicles on a highway. Considering that the road width of highways is usually much smaller than the wireless transmission range and that the curves on highways are usually not sharp, we can approximately model the group of vehicles as a 1-D linear VANET (1-DL-VANET). A similar model is adopted in [1] and [2]. Here, we consider only intervehicle communications, and thus, roadside units are not involved. In a 1-DL-VANET, some vehicles may leave or quit the current network, e.g., due to arriving at their exits on the highway or due to mechanical faults. Upon departures of those vehicles, it is desired that any two remaining vehicles can still communicate with each other. In other words, the high connectivity level of the 1-DL-VANET is desired. In specific, if there exists a one- or multiple-hop communication path between any two nodes in a network, the network is said to be *connected*; otherwise, the network is said to be *unconnected* or *disconnected*. A network is called k-*connected* if removal of any $(k-1)$ arbitrary nodes does not disconnect the network [3]. In particular, biconnectivity means that $k=2$, which is a popular connectivity measure [4]–[8].

In the literature, connectivity has been well investigated for ad hoc networks. Existing research efforts are focused on how to achieve connectivity or biconnectivity by the following: 1) setting the wireless transmission range or node density or 2) changing the network topology by adjusting transmission power or by node movement inside the network. On the other hand, research on the expression of the probability of a network being connected, biconnected, or k-connected is still in its infancy. Current limited research efforts are focused on the probability of a 1-D network being connected or biconnected.

1) The probability of a 1-D network being connected is investigated in [9]–[12]. In [9], by considering all realizable networks as in a polytope, the probability of a network being connected is derived in closed form. In [10], the probability of a network consisting of at most $C(\geq 1)$ clusters is first calculated, which is equal to the probability that the Cth largest spacing (the distance between consecutive vehicles) is smaller than the wireless communication range denoted R. In particular, when $C=1$, the probability of all spacings smaller than R is actually the probability that the network is connected. A queuing model is utilized in [11] to analyze the connectivity of 1-D networks. The exact results of the coverage probability, the node isolation probability, and the connectivity distance for several node placements are obtained. In [12], asymptotic analysis for 1-D network connectivity is obtained. It is concluded that, as the number of nodes goes to infinity, the probability of the network being connected is approximately 1 when the wireless transmission range (i.e., R) is larger than a threshold and 0 when R is smaller than that threshold.
2) In [13], the probability of a 1-D network being biconnected is approximated as the product of the probabilities of two events: the network is connected, and there are no cut nodes. (If the removal of a node makes the remaining network disconnected, the node is called a *cut node.*) The independence of the two events is validated through simulation.